Arch. Metall. Mater., Vol. 61 (2016), No 3, p. 1649–1654

DOI: 10.1515/amm-2016-0267

M. ZAMANI NEJAD*#, M. ABEDI*, M.H. LOTFIAN*, M. GHANNAD**

EXACT AND NUMERICAL ELASTIC ANALYSIS FOR THE FGM THICK-WALLED CYLINDRICAL PRESSURE VESSELS WITH EXPONENTIALLY-VARYING PROPERTIES

Assuming exponential-varying properties in the radial direction and based on the elasticity theory, an exact closed-form analytical solution is obtained to elastic analysis of FGM thick-walled cylindrical pressure vessels in the plane strain condition. Following this, radial distribution of radial displacement, radial stress, and circumferential stress are plotted for different values of material inhomogeneity constant. The displacements and stresses distributions are compared with the solutions of the finite element method (FEM).

Keywords: cylindrical pressure vessel, thick-walled, Functionally Graded Material (FGM), Finite element method (FEM), exponential

1. Introduction

Functionally graded materials (FGMs) are a new type of materials with continuously varied microstructure, which lead to the continuous variation of physical and mechanical properties through the thickness. These materials are advanced, heat resisting, erosion and corrosion resistant, and have high fracture toughness. The thick cylindrical pressure vessels made of FG materials can be used in many engineering fields such as aerospace, mechanical, naval, nuclear energy, chemical plant, electronics, and biomaterials and so on.

Horgan and Chan [1] analyzed a pressurized hollow cylinder in the state of plane strain. Assuming that the material has a graded modulus of elasticity, while the Poisson's ratio is a constant, Tutuncu and Ozturk [2], investigated the stress distribution in the axisymmetric structures. They obtained the closed-form solutions for stresses and displacements in functionally graded cylindrical and spherical vessels under internal pressure. Shi et al. [3], studied two different kinds of heterogeneous elastic hollow cylinders. One was multi-layered, and the second had continuously graded properties. They found the exact solutions for an N-layered elastic hollow cylinder subjected to uniform pressures on the inner and outer surfaces. Given the assumption that the material is isotropic with constant Poisson's ratio and exponentially varying modulus of elasticity through the thickness, Naki Tutuncu [4], obtained power series solutions for stresses and displacements in functionally-graded cylindrical vessels subjected to internal pressure alone. In a recent study by Chen and Lin [5], assuming that the property of FGMs is exponential function form, they conducted the elastic analysis for both a thick cylinder and a spherical pressure vessel which were made of functionally graded materials. Assuming that the material properties vary nonlinearly in the radial direction and the Poisson's ratio is constant, Zamani Nejad and Rahimi [6], obtained closed form solutions for one-dimensional steady-state thermal stresses in a rotating functionally graded pressurized thick-walled hollow circular cylinder. A complete and consistent 3-D set of field equations has been developed by tensor analysis to characterize the behavior of FGM thick shells of revolution with arbitrary curvature and variable thickness along the meridional direction [7]. Ghannad and Zamani Nejad [8], obtained the elastic solution of clamped-clamped thick-walled cylindrical shells by an analytic method. Assuming that the material properties vary nonlinearly in the radial direction and the Poisson's ratio is constant, Zamani Nejad and Rahimi [9] obtained closed form solutions for stresses and displacements in a rotating functionally graded pressurized thick-walled hollow circular cylinder. Assuming the volume fractions of two phases of a FG material vary only with the radius, Nie et al. [10], obtained a technique to tailor materials for linear elastic hollow cylinders and spheres to attain through the thickness either a constant circumferential stress or a constant in-plane shear stress. Based on basic equations of elasticity and power series solution method (PSSM), a simple and efficient method is proposed to elastic analysis of rotating internally pressurized thick-walled cylindrical pressure vessels in plane strain and plane stress conditions by Gharibi and Zamani Nejad [11].

In this paper, using the infinitesimal theory of elasticity, a closed-form analytical solution for displacements and stresses of FGM thick cylindrical pressure vessels with exponential varying material properties are obtained. For the numerical solution, a commercial finite element program ANSYS 12 is used.

* MECHANICAL ENGINEERING DEPARTMENT, YASOUJ UNIVERSITY, P.O.BOX: 75914-353, YASOUJ, IRAN

** MECHANICAL ENGINEERING FACULTY, UNIVERSITY OF SHAHROOD, SHAHROOD, IRAN

Corresponding author: m.zamani.n@gmail.com

2. Problem formulation

Consider a thick cylindrical pressure vessel with an inner radius a, and an outer radius b, subjected to internal and external pressure P_i and P_o, respectively. (Fig. 1).

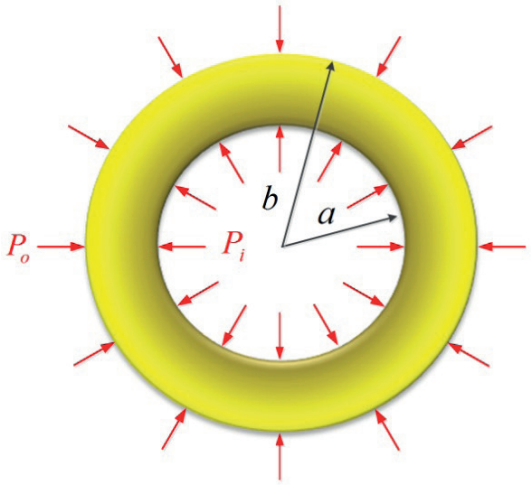

Fig. 1. Configuration of an FGM thick cylindrical pressure vessel

It is assumed that the Poison's ratio υ, takes a constant value, because its variation has much less practical significance than that of the elasticity modulus, and the modulus of elasticity E, is assumed to vary radially according to exponential form as follows,

$$\begin{cases} E(R) = E_i e^{\ln(\xi)\frac{1-R^\eta}{1-K^\eta}} \\ \xi = \dfrac{E_o}{E_i} \\ K = \dfrac{b}{a} \\ R = \dfrac{r}{a} \end{cases} \tag{1}$$

Here, E_i and E_o are modulus of elasticity in inner and outer surfaces, respectively. ξ and η are inhomogeneity parameters.

Radial and circumferential strains (ε_r, ε_θ), in the polar coordinates are as follows,

$$\varepsilon_r = \frac{du}{dr} \tag{2}$$

$$\varepsilon_\theta = \frac{u}{r} \tag{3}$$

where u is radial displacement.

The stress-strain relations for non-homogenous and isotropic materials are

$$\begin{pmatrix} \sigma_r \\ \sigma_\theta \end{pmatrix} = \frac{E(R)}{a}\begin{pmatrix} A & B \\ B & A \end{pmatrix}\begin{pmatrix} \dfrac{du}{dR} \\ \dfrac{u}{R} \end{pmatrix} \tag{4}$$

where σ_r and σ_θ are radial and circumferential stresses. A and B are related to Poisson's ratio υ as

$$\begin{cases} A = \dfrac{1-\upsilon}{(1+\upsilon)(1-2\upsilon)} \\ B = \dfrac{\upsilon}{(1+\upsilon)(1-2\upsilon)} \end{cases} \tag{5}$$

The equilibrium equation in the absence of body forces, is expressed as

$$\frac{d\sigma_r}{dR} + \frac{\sigma_r - \sigma_\theta}{R} = 0 \tag{6}$$

Substituting Eqs. (4), into Eq. (6), the equilibrium equation is expressed as

$$\begin{cases} R^2\dfrac{d^2u}{dR^2} + R\left(1+\dfrac{RE'}{E}\right)\dfrac{du}{dR} - \left(1-\upsilon^*\dfrac{RE'}{E}\right)u = 0 \\ \upsilon^* = \dfrac{B}{A} = \dfrac{\upsilon}{1-\upsilon} \end{cases} \tag{7}$$

here, prime denotes differentiation with respect to R. The general solution of Eq. (7) is as follows

$$u(R) = C_1 G(R) + C_2 H(R) \tag{8}$$

where C_1 and C_2 are arbitrary integration constants. Here G and H are homogeneous solutions.

Substituting Eq. (8) into Eqs. (4), yields

$$\begin{pmatrix} \sigma_r \\ \sigma_\theta \end{pmatrix} = \frac{E(R)}{a}\begin{pmatrix} A & B \\ B & A \end{pmatrix}\begin{pmatrix} C_1 G' + C_2 H' \\ C_1\dfrac{G}{R} + C_2\dfrac{H}{R} \end{pmatrix} \tag{9}$$

The forms of G and H will be determined next.

Substituting Eq. (1) into Eq. (7), the governing differential equation is as follows

$$R^2\frac{d^2u}{dR^2} + R\left(1-\eta n R^\eta\right)\frac{du}{dR} - \left(1+\upsilon^*\eta n R^\eta\right)u = 0 \tag{10}$$

Eq. (10) is a homogeneous hypergeometric differential equation.

Using a new variable $x = nR^\eta = \left(\ln(\xi)/\left(1-K^\eta\right)\right)R^\eta$ and applying the transformation $u(R) = Ry(x)$, the result Eq. (10) is

$$x\frac{d^2y}{dx^2} + \left(1+\frac{2}{\eta}-x\right)\frac{dy}{dx} - \frac{1+\upsilon^*}{\eta}y = 0 \tag{11}$$

The solution of Eq. (11) is given as

$$y(x) = C_1 F_C(\alpha,\beta;x) + \bar{C}_2 x^{-2/\eta} F_C(\alpha-\beta+1,2-\beta;x) \tag{12}$$

With $F_C(\alpha,\beta;x)$ being the hypergeometric function defined by Abramowitz and Stegun [11],

$$F_C(\alpha,\beta;x)=1+\sum_{k=1}^{\infty}\frac{(\alpha)_k}{(\beta)_k}\frac{x^k}{k!} \tag{13}$$

where

$$(\alpha)_k=\alpha(\alpha+1)\cdots(\alpha+k-1) \tag{14}$$

Thus

$$F_C(\alpha,\beta;x)=1+\frac{\alpha}{\beta}\frac{x}{1!}+\frac{\alpha(\alpha+1)}{\beta(\beta+1)}\frac{x^2}{2!}+\frac{\alpha(\alpha+1)(\alpha+2)}{\beta(\beta+1)(\beta+2)}\frac{x^3}{3!}+\cdots \tag{15}$$

In Eq. (15), the arguments α and β are determined as

$$\begin{cases}\alpha=\dfrac{1+\upsilon^*}{\eta}\\ \beta=1+\dfrac{2}{\eta}\end{cases} \tag{16}$$

From $u(R)=Ry\left(nR^{\eta}\right)$, the homogeneous solutions G and H are found in the form

$$\begin{cases}G(R)=RF_C\left(\alpha,\beta;nR^{\eta}\right)\\ H(R)=\dfrac{1}{R}F_C\left(\alpha-\beta+1,2-\beta;nR^{\eta}\right)\end{cases} \tag{17}$$

The Eqs. (8) and (9) may be rewritten with non-dimensional parameters as

$$U(R)=C_3G(R)+C_4H(R) \tag{18}$$

$$\begin{pmatrix}\bar{\sigma}_r\\ \bar{\sigma}_\theta\end{pmatrix}=e^{\ln(\xi)\frac{1-R^{\eta}}{1-K^{\eta}}}\begin{pmatrix}A & B\\ B & A\end{pmatrix}\begin{pmatrix}C_3G'+C_4H'\\ C_3\dfrac{G}{R}+C_4\dfrac{H}{R}\end{pmatrix} \tag{19}$$

where

$$U=\frac{uE_i}{aP_i},\ \bar{\sigma}=\frac{\sigma}{P_i},\ \frac{C_3}{C_1}=\frac{C_4}{C_1}=\frac{E_i}{aP_i} \tag{20}$$

Integration constants C_3 and C_4 are determined by using the following boundary conditions

$$\begin{cases}\bar{\sigma}_r(R=1)=-1\\ \bar{\sigma}_r(R=K)=-P\\ P=\dfrac{P_o}{P_i}\end{cases} \tag{21}$$

Thus

$$\begin{cases}\left[AG'(1)+BG(1)\right]C_3+\left[AH'(1)+BH(1)\right]C_4=-1\\ \left[AG'(K)+B\dfrac{G(K)}{K}\right]C_3+\left[AH'(K)+B\dfrac{H(K)}{K}\right]C_4=-\dfrac{P}{\xi}\end{cases} \tag{22}$$

Using Eqs. (22), the constants C_3 and C_4 are determined as follows

$$\begin{cases}C_3=\dfrac{D_2D_5+D_4}{D_2D_3-D_1D_4}\\ C_4=\dfrac{D_1D_5+D_3}{D_1D_4-D_2D_3}\end{cases} \tag{23}$$

Where

$$\begin{cases}D_1=AG'(1)+BG(1)\\ D_2=AH'(1)+BH(1)\\ D_3=AG'(K)+B\dfrac{G(K)}{K}\\ D_4=AH'(K)+B\dfrac{H(K)}{K}\\ D_5=-\dfrac{P}{\zeta}\end{cases} \tag{24}$$

Hence, the radial displacement, radial stress, and circumferential stress are as follows

$$U(R)=\frac{Q_1G(R)-Q_2H(R)}{Q_0} \tag{25}$$

$$\bar{\sigma}_r(R)=\frac{Q_1}{Q_0}\Big\{A\left[G'(R)-H'(R)\right]+\frac{B}{R}\left[G(R)-H(R)\right]\Big\}e^{\ln(\xi)\frac{1-R^{\eta}}{1-K^{\eta}}} \tag{26}$$

$$-(R)=\frac{Q}{Q}\left\{\frac{A}{R}\left[G(R)-H(R)\right]B\left[G'(R)-H'(R)\right]\right\}e^{\ln(\xi)\frac{1-R^{\eta}}{1-K^{\eta}}} \tag{27}$$

where

$$Q_0=A^2\left[G'(K)H'(1)-G'(1)H'(K)\right]+B^2\left[\frac{G(K)H(1)-G(1)H(K)}{K}\right]+AB\left[G'(K)H(1)-G'(K)H(1)+\frac{G(K)H'(1)-G'(1)H(K)}{K}\right] \tag{28a}$$

$$Q_1=A\left[H'(K)-\frac{P}{\xi}H'(1)\right]+B\left[H(K)-\frac{P}{\xi}H(1)\right] \tag{28b}$$

$$Q_2=A\left[G'(K)-\frac{P}{\xi}G'(1)\right]+B\left[G(K)-\frac{P}{\xi}G(1)\right] \tag{28c}$$

3. Numerical analysis

In this study in order to numerical analysis of problem, a geometry specimen was modelled using a commercial finite elements code, ANSYS 12, for a comparative study. In the FE model, due to symmetry, only a quarter of the cylindrical pressure vessel was considered. An 8-node axisymmetric quadrilateral element was used to represent the FGM specimen. For modelling of FGM cylindrical pressure vessel, the variation in material properties was implemented by 40 layers, with each layer having a constant value of material properties. Fig. 8 illustrates the meshing region. The nodal points along the horizontal edge passing through the center were free to move in X direction but were constrained from moving in the Y direction to reflect the symmetry of cylinder specimen geometry.

In the finite element model, input dada are as follows

$$\begin{cases} P_i = 80MPa \quad , \quad E_i = 200GPa \quad , \quad \upsilon = 0.3 \\ a = 40mm \quad , \quad b = 60mm \end{cases} \tag{29}$$

4. Results and discussion

The analytical solution described in the preceding section for a thick cylindrical pressure vessel with $b=1.5a$, $P_i=P_o$ and $\upsilon = 0.3$ is considered.

For different values of ξ and η, dimensionless modulus of elasticity along through the radial direction is plotted in Fig. 2. According to this figure, at the same position ($1<R<1.5$), for $\xi=1.5$, dimensionless modulus of elasticity increases as η decreases, while for $\xi=0.5$, the reverse holds true.

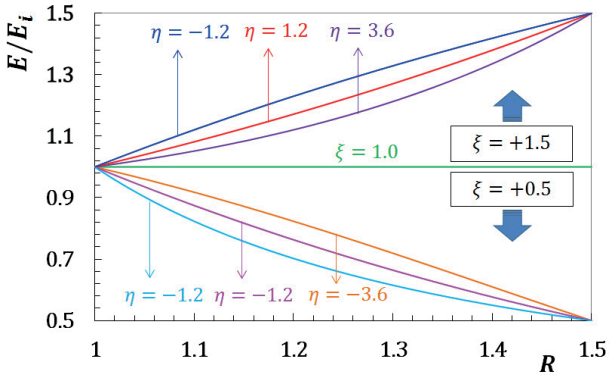

Fig. 2. Radial distribution of modulus of elasticity

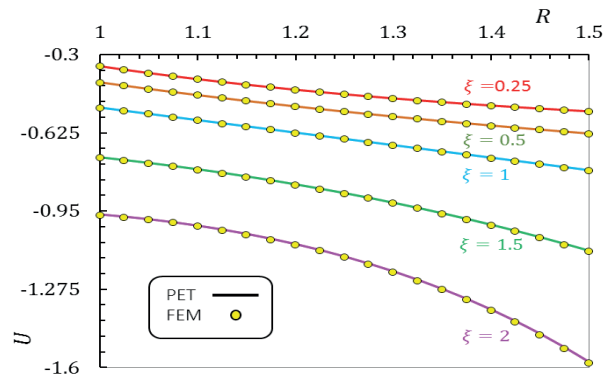

Fig. 3. Radial distribution of radial displacement

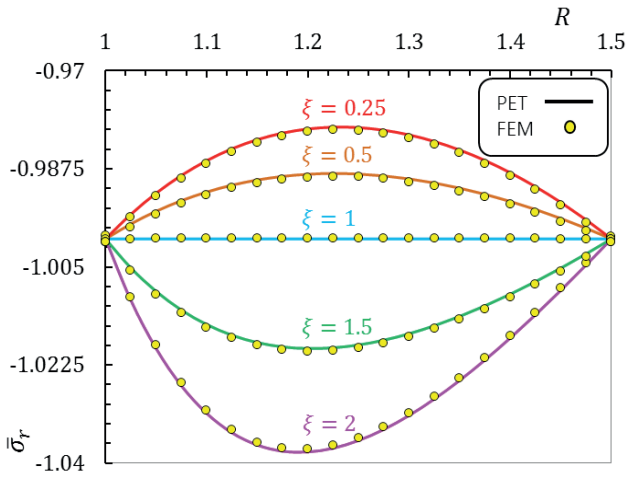

Fig. 4. Radial distribution of radial stress

Figs. 3 and 4 show plots of the radial displacement and the radial stress along the radial direction for different values of ξ and $\eta=1.2$. From these figures it is observed that at the same position ($1<R<1.5$), for higher values of ξ, radial displacement and radial stress decrease.

The circumferential stress along the radial direction for different values of ξ and $\eta=1.2$ is plotted in Fig. 5. It must be noted from this figure that at the same position, almost for $R \approx 1.23$, there is an decrease in the value of the circumferential stress as ξ increases, whereas for $R<1.23$ this situation was reversed. Besides, along the radial direction for the $\xi>1$, circumferential stress increases, while for $\xi>1$, the circumferential stress decreases.

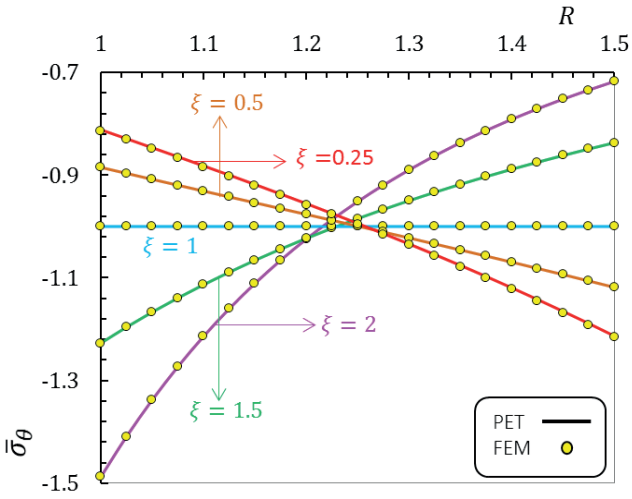

Fig. 5. Radial distribution of circumferential stress

In Figs. 6 and 7, radial displacement and stresses using values $\xi=0.5$ and $\eta=3.6$ is calculated and compared to those in a homogeneous thick-walled cylindrical pressure vessel ($\xi=1$).

The radial displacements, radial stresses, and circumferential stresses values for $\xi=0.6$ and $\eta=1.2$ is obtained from ANSYS commercial finite elements analysis program and their numerical results are depicted in Figs. 9 to 11.

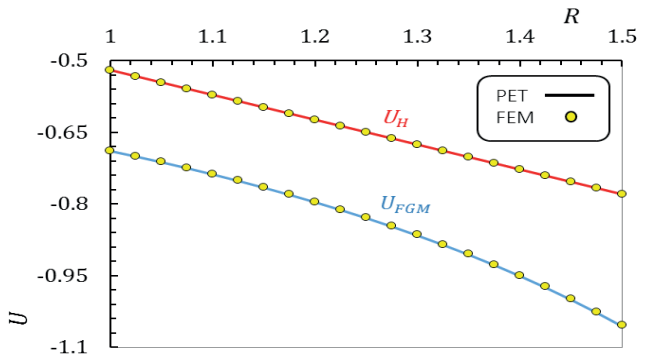

Fig. 6. Comparison of radial displacement in an FGM thick-walled cylindrical pressure vessel to those in homogeneous thick-walled cylindrical pressure vessel

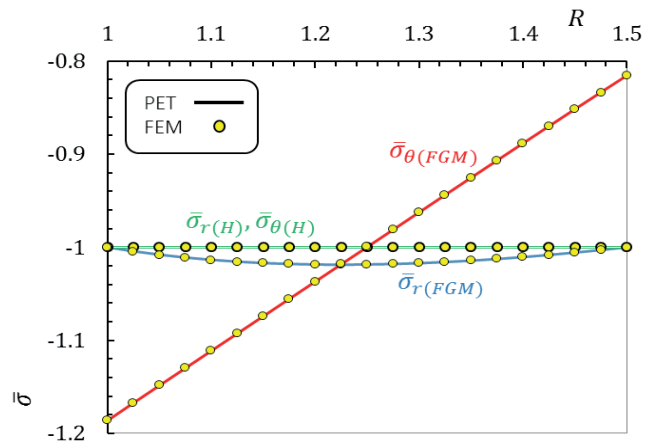

Fig. 7. Comparison of radial stress in an FGM thick-walled cylindrical pressure vessel to those in homogeneous thick-walled cylindrical pressure vessel

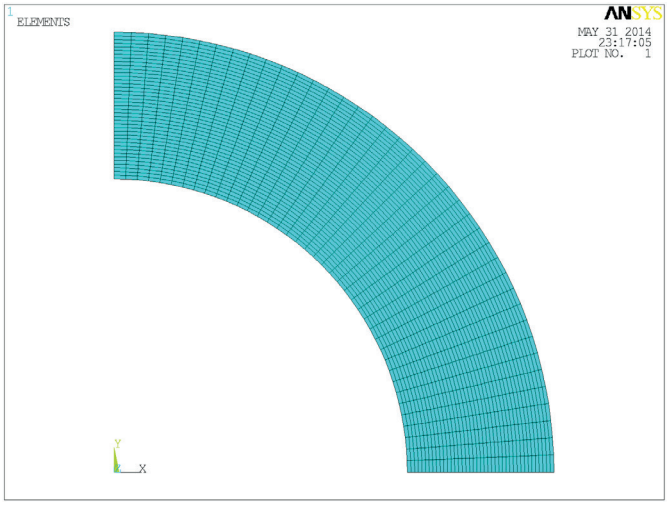

Fig. 8. Finite elements mesh region from ANSYS code

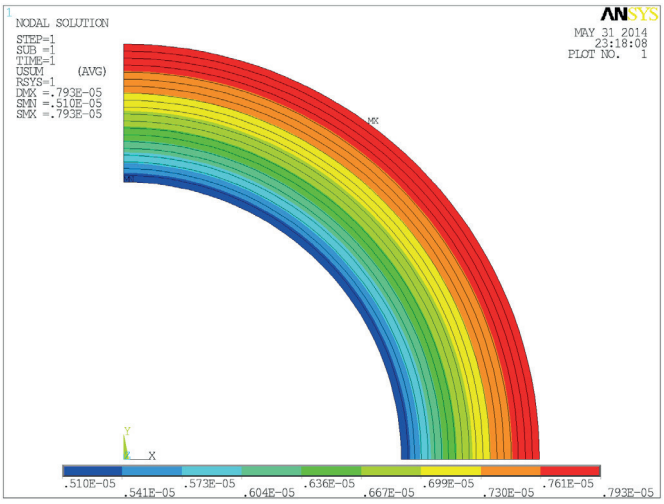

Fig. 9. Radial displacement obtained from ANSYS code

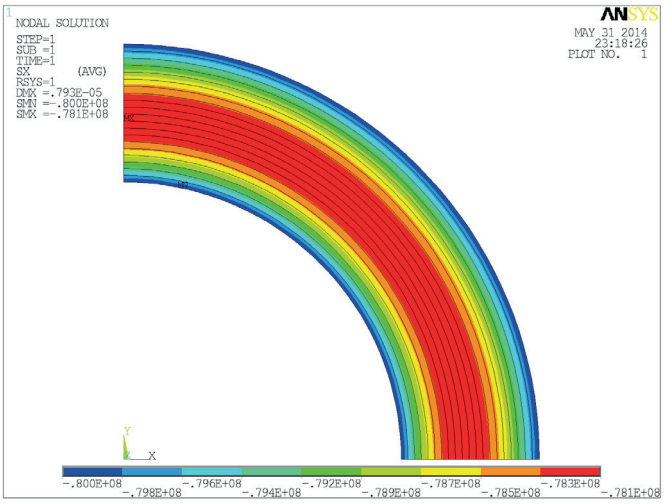

Fig. 10. Radial stress obtained from ANSYS code

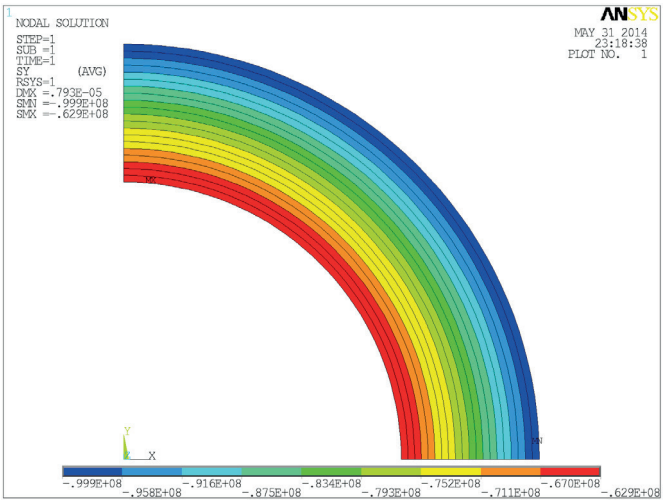

Fig. 11. Circumferential stress obtained from ANSYS code

5. Conclusion

In this work, using a mathematical method, an elastic analysis for FGM thick cylindrical pressure vessels with exponential varying material properties in the plane strain condition is presented. The method presented is very suitable for the purpose of calculation of radial displacement, radial stress, and circumferential stress. To show the effect of inhomogeneity on the stress distributions, different values were considered for material inhomogeneity parameter ζ. The presented results show that the material inhomogeneity has a significant influence on the mechanical behaviors of exponential FGM thick-walled cylindrical pressure vessels. In the present study, from ANSYS commercial finite elements analysis program, a numerical solution is also presented. Good agreement was found between the analytical solutions and the solutions carried out through the FEM. It is also possible to find an optimum value for the inhomogeneity parameter such that the variation of stresses along the radial direction is minimized, yielding optimum use of material.

REFERNCES

[1] C.O. Horgan, A.M. Chan, J Elast. **55**, 43 (1999).
[2] N. Tutuncu, M. Ozturk, Compos Part B-Eng. **32**, 683 (2001).
[3] Z.F. Shi, T.T. Zhang, H.J. Xiang, Compos Struct. **79**, 140 (2007).
[4] N. Tutuncu, Eng Struct. **29**, 2032 (2007).
[5] Y.Z. Chen, X.Y. Lin, Comp Mater Sci. **44**, 581 (2008).
[6] M.Z. Nejad, G.H. Rahimi, Sci Res Essays. **4**, 131 (2009).
[7] M.Z. Nejad, G.H. Rahimi, M. Ghannad, Mechanika. **77**, 18 (2009).
[8] M. Ghannad, M.Z. Nejad, Mechanika. **85**, 11 (2010).
[9] M.Z. Nejad, G.H. Rahimi, J Chin Inst Eng. **33**, 525 (2010).
[10] G.J. Nie, Z. Zhong, R.C. Batra. Compos Sci Technol. **71**, 666 (2011).
[11] M. Abramowitz, A.I. Stegun (eds.), Handbook of Mathematical Functions. Washington, D.C.: US Government Printing Office 1966.